

Modeling analysis of the mean flow velocity ahead of a rotating tidal turbine

Ph. Druault and J-F. Krawczynski

Abstract—This paper presents a novel method for modeling the mean radial velocity component ahead of a rotating tidal turbine. Firstly, it examines a recent hybrid model designed to reconstruct the three-dimensional mean axial flow field in front of an operating turbine under various flow conditions (uniform, shear) and rotational speeds (thrust turbine coefficient). Subsequently, based on the continuity equation and the axial velocity reconstruction on a meshgrid, a new turbine induction model is proposed to model the mean velocity component. The model is validated against experimental data under both uniform and shear flow conditions, showing excellent agreement between the modeling and experimental results, with minor discrepancies near the blade tips. The proposed method provides a useful tool to evaluate the induction effect in front of a rotating turbine by considering the characteristics of the incoming average flow field.

Index Terms—Tidal turbine induction, Analytical modeling, Full mean velocity reconstruction

I. INTRODUCTION

SIGNIFICANT non-uniformities in the inflow, either due to the complex boundary layer developing over the bathymetry, partial wake conditions from an upstream turbine, or turbulence, are common operational conditions for tidal turbines. In addition, a rotating turbine generates regions of reduced flow velocity both downstream (wake) and upstream (induction zone) where the characteristics of the complex incoming flow are altered up to several diameters upstream of both wind turbines [1], [2] and tidal turbines [3], [4]. An in-depth grasp of the so-called induction zone that is, the disturbed flow which actually interacts with the turbine, is crucial for enhancing device design, turbine array reliability, and energy conversion efficiency.

Accurately accounting for these inflow conditions in the rotor aerodynamic models for turbine design load calculations remains a highly challenging task. Where high-fidelity computation fluid dynamics (CFD)

still fails to meet the requirements in terms of computational cost, the fast engineering blade-element momentum (BEM) model, widely used in the aeroelastic codes of the industry, is still questionable in non-uniform inflow conditions which violate several of its assumptions. This motivates the seek for a modeling approach, in a version where the induction will vary as a function of the blade radial and azimuthal positions and will be correlated with the free-stream velocity.

To derive a simple analytical model for the streamwise velocity upstream of a wind turbine, regardless of blade design, Reynolds Average Navier-Stokes (RANS) simulations were conducted to study the induction zone upstream of various wind turbine rotors in steady uniform inflow [5]. The results indicated that the induction zone is self-similar for distances greater than one turbine radius upstream of the rotor, leading to the development of the self-similar induction (SSI) model, which is applicable beyond this distance upstream of any (wind-) rotor plane.

Recently, the mean axial velocity field in front of a rotating scaled tidal turbine was experimentally examined and compared with consolidated induction models [6]. The study found that including the hub separately in the analytical turbine induction model significantly improved the description of the streamwise velocity deficit upstream of an operating tidal turbine. This improvement is related to the hub-to-turbine diameter ratio, which is higher for tidal turbines than for wind turbines.

This study aims to extend these developments to fully characterize the mean velocity field upstream of a tidal turbine.

It is important to note that the mean radial velocity component has been studied less extensively than the axial component and is frequently overlooked due to its *a priori* relatively low amplitude. Under the influence of an incoming vertical shear axial velocity field with a negligible radial component $U_{r,free} \approx 0$, the mean radial velocity component of the velocity deficit was found to exhibit an asymmetric shear profile along the vertical direction ahead of the turbine [3]. In addition, this component exhibited notable values, particularly at the tip of the blade relative to the mean axial velocity component. Therefore, the radial component of the velocity field in front of a rotating turbine needs to be further investigated.

The remainder of this paper is organized as follows: First, we introduce a new approach to modeling the velocity field upstream of a tidal turbine. Next, we extend this approach to provide a three-dimensional characterization of the velocity deficit. We then conduct

Part of a special issue for AWTEC 2024. Manuscript submitted 27 September 2024; Revised 3 June 2025; Accepted 26 June 2025. Published 20 October 2025.

This is an open access article distributed under the terms of the Creative Commons Attribution 4.0 International license. CC BY <https://creativecommons.org/licenses/by/4.0/>. Unrestricted use (including commercial), distribution and reproduction is permitted provided that credit is given to the original author(s) of the work, including a URI or hyperlink to the work, this public license and a copy right notice. This article has been subject to a single-blind peer review by a minimum of two reviewers.

Ph. Druault and J-F. Krawczynski are from Sorbonne Université, CNRS, Institut Jean Le Rond d'Alembert, F-75005 Paris, France (e-mail: philippe.druault@sorbonne-universite.fr, jean-francois.krawczynski@sorbonne-universite.fr.)

Digital Object Identifier:
<https://doi.org/10.36688/imej.8.359-366>

a thorough analysis of the mean radial velocity component, examining a turbine's performance at various rotational speeds and under different mean vertical axial velocity shears. Finally, we critically compare the proposed analytical model with the experimental data.

II. MODELING

Throughout this paper, we refer to the mean axial and radial components of the velocity field as $U(r, x, \theta)$ and $U_r(r, x, \theta)$, respectively. Here, the x axis represents the stream-wise direction, whereas the radial direction lies within the (y, z) plane, with y as the cross-flow coordinate and z as the vertical coordinate. The origin $r = 0$ or $z = 0$ lies along the rotational axis of the hub. Furthermore, the term free mean velocity $U_{\text{free}}(r, x, \theta)$ is used to describe the velocity field of the flow in the absence of a turbine. This velocity is presumed to be known and uniform along the y direction.

A. The mean axial velocity component

Various induction models are available to estimate the mean axial component of the velocity field upstream of an operating turbine. These models were originally designed for wind turbines [7], with recent adaptations proposed for tidal turbines [4], [6]. For the last case, where the ratio of the hub to the rotor diameters is much more important than for wind turbines, the additional induction due to the tidal hub was not properly considered. To address this limitation, we proposed pairing two models: the self-similar induction (SSI) model [5] and the hub model [8] to assess the mean axial flow ahead of the rotating blades and ahead of the hub, respectively [6]

$$U(x, r, \theta) = U_{\text{free}}(x, r, \theta) + U_{\text{hub}} + \langle U \rangle U_{\text{SSI}}(x, r). \quad (1)$$

where $\langle U \rangle$ is the spatially averaged velocity over the rotor area. The basic principles to derive this model are briefly outlined in the appendices. For more detailed information, the interested reader is invited to refer to the aforementioned paper.

The subsequent proposal aims to enhance this model to represent the three-dimensional mean axial flow field approaching a rotating tidal turbine.

B. The mean radial velocity field

Very few attempts have tried to model the radial component of the velocity field in front of a rotating tidal turbine. Unlike the modeling of the axial component of the velocity field, which can be derived from the axial momentum theory, it is not possible to obtain a direct modeling of the radial component of the velocity deficit. Therefore, for wind turbines, it has been suggested to apply the analytical solution for the radial velocity of a two-dimensional actuator disc with modifications to align with current Actuator Disc (AD) results for an axisymmetric disc [13]:

$$U_r(r) = \frac{U_{\text{free}} C_t}{2.24 \cdot 4\pi} \ln \left(\frac{0.04^2 + (r+1)^2}{0.04^2 + (r-1)^2} \right) \quad (2)$$

This model was developed in the context of wind turbines under assumptions (uniform flow, actuator disc model) that may not be suitable for tidal turbines.

We introduce an alternative approach based on the modeling of the mean axial velocity deficit previously introduced. Therefore, we choose to derive a model based on the integration of the continuity equation written under the assumptions of axisymmetry and incompressibility:

$$U_r(r, x, \theta) = -\frac{1}{r} \int_r^{\infty} r' \frac{\partial U(x, r, \theta)}{\partial x} (x, r') dr', \quad (3)$$

where $U(x, r, \theta)$ is given by (1).

Since the three terms in the RHS of (1) are linearly independent, we use the formulation of [8] based on the potential flow theory to express the blockage effect of the hub on the radial component of the velocity field,

$$U_{r,\text{hub}}(x, r) = \frac{\partial \phi}{\partial \mu} \frac{\partial \mu}{\partial r} + \frac{\partial \phi}{\partial \xi} \frac{\partial \xi}{\partial r} \quad (4)$$

where (μ, ξ) are the semi-elliptic coordinates as introduced in the appendix.

The SSI model was designed assuming self-similarity of the induced flow, that is the mean axial velocity component is assumed to be written as [5]

$$U_{\text{SSI}} = U_c(x) f(\zeta) \quad (5)$$

with $\zeta = r/\mathcal{L}$, $\mathcal{L} \equiv r_{1/2}(x)$. After some basic calculation, the radial counterpart to the axial induction can be analytically evaluated from (3) as

$$U_r(x, \zeta) = -\mathcal{L} \frac{\partial U_c}{\partial x} \int_0^\zeta f(\zeta') d\zeta' + U_c \frac{\partial \mathcal{L}}{\partial x} \int_0^\zeta f(\zeta') \frac{\partial f}{\partial \zeta'}(\zeta') d\zeta', \quad (6)$$

where the functions $U_c(x)$ and $\mathcal{L}(x)$ are assumed to be smooth functions of x . The explicit dependence on x of the functions $U_c(x)$ and $\mathcal{L}(x)$ and their derivatives has been omitted from the above expression for the sake of conciseness. The function $f(\zeta)$ is defined as

$$f(\zeta) = \text{sech}^\alpha(\beta\zeta) = \left(\frac{2}{e^{\beta\zeta} + e^{-\beta\zeta}} \right)^\alpha, \quad (7)$$

with parameters $\alpha > 0$ and $\beta > 0$. The integrals in Eq. (6) involve the function $f(\zeta)$ and its product with its derivative. Although $\text{sech}^\alpha(\beta\zeta)$ has elementary antiderivatives only for special values of α , the general case does not admit closed-form solutions. Moreover, the second integral involves a nonlinear product $f(\zeta) \partial f / \partial \zeta$, further complicating any analytical attempt. To obtain a tractable and accurate approximation, we expand the integrands in Taylor series about $\zeta = 0$, enabling term-by-term integration.

In the following, both modeling methods (equations 2 and 6) are compared with the available experimental data.

III. RESULTS

A. 3-D reconstruction of the mean axial velocity component

In the following, the three-dimensional reconstruction of the mean axial velocity component in the turbine induction area is carried out successively using (17) for different test cases: uniform incoming flow

with several thrust coefficients and incoming shear flow at a constant thrust coefficient. Some parameters for the formulation of the model are chosen in accordance with previous experiments [3], [9] carried out in the IFREMER wave and current circulating flume tank located in Boulogne-sur-Mer (France).

a) Incoming uniform flow:

We consider an incoming uniform velocity field with $U_{\text{free}} = 0.88$ m/s and three values for the thrust coefficients: $C_t = 0.96$, $C_t = 0.7$ and $C_t = 0.36$ [3]. A three-dimensional Cartesian domain of dimensions $(L_x, L_y, L_z) = (R, 2R, 2R)$, with R the rotor radius of the turbine, corresponding to a mesh size of 100 points in each direction, is retained. Note that the x -origin represents the point where the blades are attached to the hub. The dimensions of the experimental scaled turbine are reproduced with $D = 2 \times R = 0.724$ m the diameter of the rotor and $R_{\text{hub}} = 0.13$ m the radius of the hub.

Figure 1 illustrates this three-dimensional reconstruction for selected z -planes ($z^* = z/R = 0, -0.5, -1$) superimposed on selected y -planes ($y^* = z/R = 0, 0.5$). In figure 3, the mean velocity reconstruction is also plotted in the $y = 0$ plane.

As the incoming flow is uniform, the reconstructed velocity field is axisymmetric in front of the turbine, regardless of the value of the thrust coefficient. Moreover, as expected, the higher the thrust coefficient, the greater the axial velocity deficit. These predictions are in agreement with previous experimental results [2]. Tidal turbines are observed to have a significantly higher hub radius ratio R_{hub}/R compared to wind turbines. Our hybrid model (17) accurately represents the specific impact of the hub on the induced velocity field.

b) Incoming shear flow:

We now consider an upstream shear velocity field in front of the operating turbine:

$$U_{\text{free}}(z) = Kz^{1/\alpha}. \quad (8)$$

The parameter K is adjusted so that the spatial average over the rotor area of the mean axial velocity remains unchanged regardless of α . The values $\alpha = 1, 2$, and 3 are used.

Figure 2 illustrates this three-dimensional reconstruction for selected z -planes ($z^* = z/R = 0, -0.5, -1$) superimposed on selected y -planes ($y^* = z/R = 0, 0.5$) for the three shear velocity profiles. Figure 4 presents the associated reconstruction in the $y = 0$ plane.

The influence of shear on induction is evident in contrast to the reconstruction of a uniform velocity field (refer to Figure 3). Specifically, the velocity deficit is no longer symmetrical relative to the hub axis. However, near the hub, the velocity deficit is identical in all three cases. This is related to the fact that in this region, the hub modeling part is the main contribution to the velocity deficit assessment. Furthermore,

it should be recalled that $U_{\text{free}}(z = 0) = 0.88$ m/s is imposed for the three shear flows. However, moving further upstream along the $z = 0$ axis, the influence of shear is evident: the upstream velocity decreases with increasing shear. Globally, the axial velocity field is recovered in agreement with previous experimental results [3], [10].

B. Validation of the radial velocity modeling

a) Incoming uniform flow:

A scale horizontal axis tidal turbine was positioned in a low-disturbance uniform flow and velocity measurements were obtained along a vertical line ($x_0 = -0.07 \times D = -0.05$ m) upstream of the rotating turbine [4]. The experiments were carried out for three configurations with Tip Speed Ratios ($TSR = 3, 4$ and 5), where $TSR = 4$ is the nominal functioning point.

Figure 5 presents the mean velocity components (U and U_r) against the radial variable in x_0 , comparing the free flow field (without turbine) with the mean velocities of the three test cases. As the tip speed ratio (TSR) increases, it leads to an amplification of the aerodynamic forces, which, in turn, reduces the axial velocity in front of the rotating turbine.

First, as in an incoming uniform axial flow, the mean radial velocity component is null, then in the induction area of a rotating turbine, the radial velocity deficit transitions to a sheared profile dependent on r [4], [11], [12]. This profile is generally symmetric with respect to the rotational axis of the hub and the amplitude of the radial velocity component increases with r due to the accelerated bypass flow. An increase in turbine rotational speed leads to greater expansion, which raises the values of U_r near the tip of the blade. Experiments revealed that the maximum value of U_r occurs around $r \sim 0.9R - 0.95R$, attributed to the onset of the tip vortex [3], [11].

The turbine thrust coefficient determined in each test case [4] will be used as input data for the velocity modeling. Furthermore, the free velocity field will be also considered for the numerical modeling of the axial velocity (equation 1) which is required for the radial velocity modeling (6).

Figure 6 presents the mean radial velocity component evaluated as given by (2) and (6) superimposed on the experimental data for the three turbine rotational configurations. First, Madsen's model (2) is not suitable for these particular data. The observed radial velocity values are significantly higher than the experimental ones. This can be attributed to the fact that this model is based on numerical AD results and does not account for the dependence x .

In contrast, there is close agreement until $r/R = 0.6$ for $TSR3$, after which the model (6) underpredicts experimental results. For $r/R < 0.5$, the experimental results match, while the numerical model shows an increase in U_r .

Furthermore, the present model cannot correctly reproduce the maximum radial velocity values observed

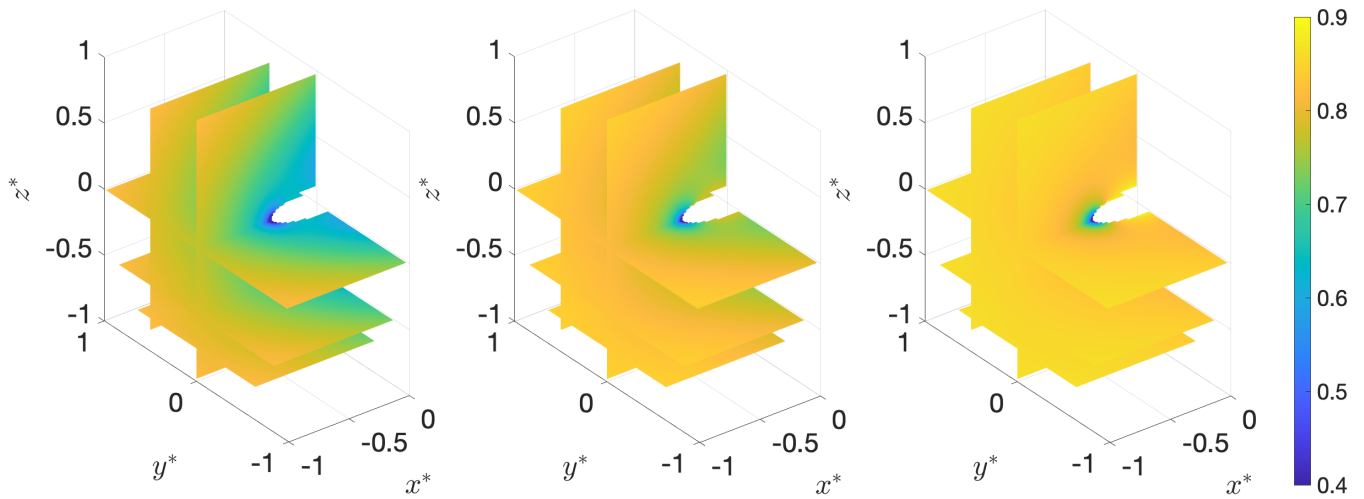


Fig. 1. Three-dimensional representation of the mean axial velocity field according to (17). Incoming uniform flow $U_\infty = 0.88 \text{ m s}^{-1}$. From left to right: $C_t = 0.96$, $C_t = 0.70$, and $C_t = 0.40$.

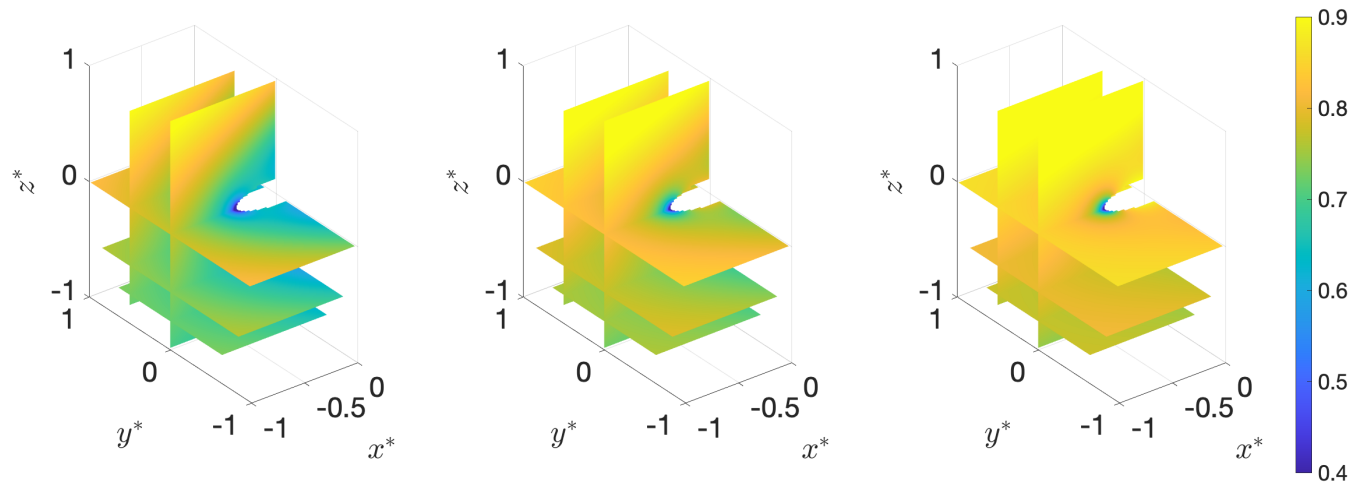


Fig. 2. Three-dimensional representation of the mean axial velocity field according to (17). Incoming shear velocity profile $Cz^{1/\alpha}$. $C_t = 0.96$. From left to right: $\alpha = 3$, $\alpha = 2$, and $\alpha = 1$.

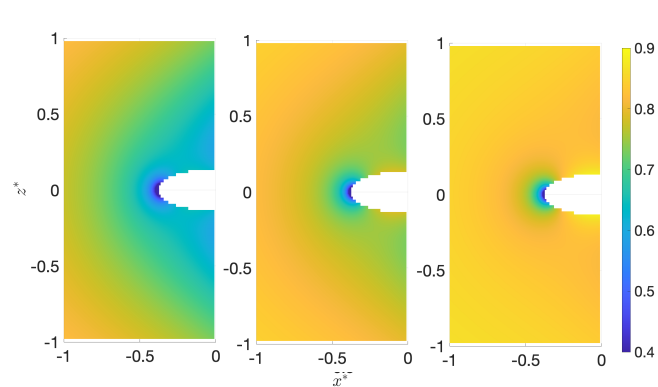


Fig. 3. Two-dimensional representation of the mean axial velocity field according to (17). Incoming uniform flow $U_\infty = 0.88 \text{ m s}^{-1}$. From left to right: $C_t = 0.96$, $C_t = 0.70$, and $C_t = 0.40$.

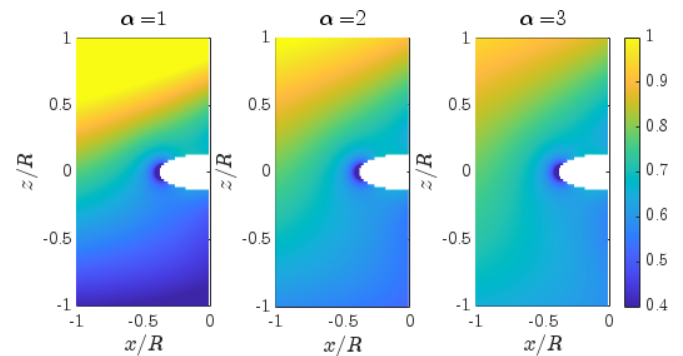


Fig. 4. Two-dimensional representation ($y = 0$ plane) of the mean axial velocity field according to (17). Incoming shear velocity profile $Cz^{1/\alpha}$. $C_t = 0.96$. From left to right: $\alpha = 1$, $\alpha = 2$, and $\alpha = 3$.

near the tip of the blade ($\sim 0.9R$ [3], [11]). This result is directly related to the axial velocity modeling and/or to the blade geometry. Minor discrepancies emerge at higher TSR levels. This is likely due to the increased turbine rotational speeds, which enhance the three-dimensional flow characteristics, thereby violating the

axisymmetry assumption. In addition, the self-similar induction (SSI) model (1) is invalid near the rotor [5], which introduces uncertainties in the prediction of radial velocity in this region.

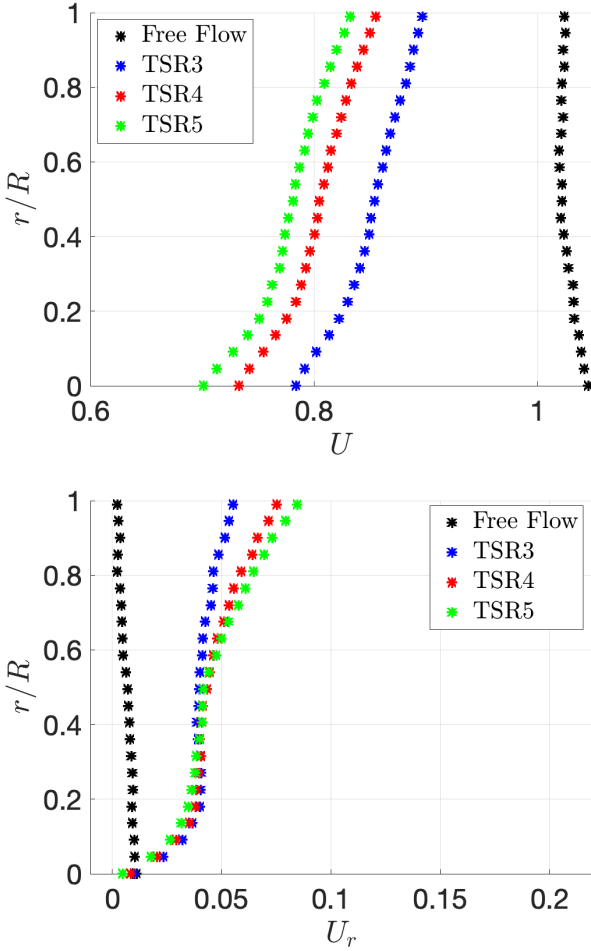


Fig. 5. Mean free velocity components superimposed to the associated mean velocities obtained in front of the turbine which operates at three different TSRs [4].

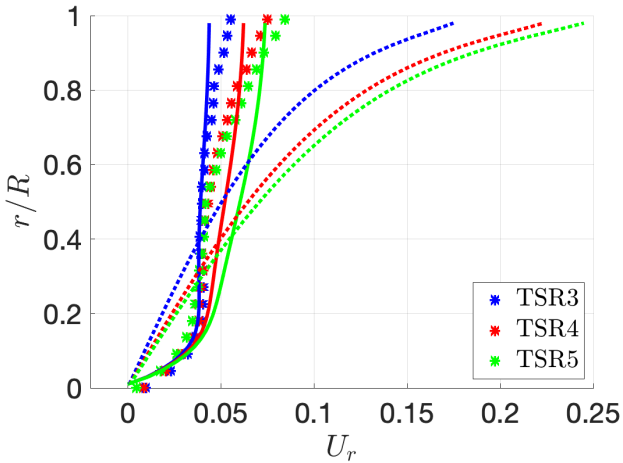


Fig. 6. Mean radial velocity modeling in presence of an incoming uniform flow. Comparison with previous published experimental data [4]. Full and dashed line: radial velocity modeling using equation (6) and (2) respectively.

b) Incoming shear flow:

In this section, we assess the robustness of the radial velocity modeling under shear conditions using previously published experimental data [3] along a vertical line ($x_0 = -0.07 \times D = -0.05$ m) upstream of the rotating turbine. The experimental setup is presented

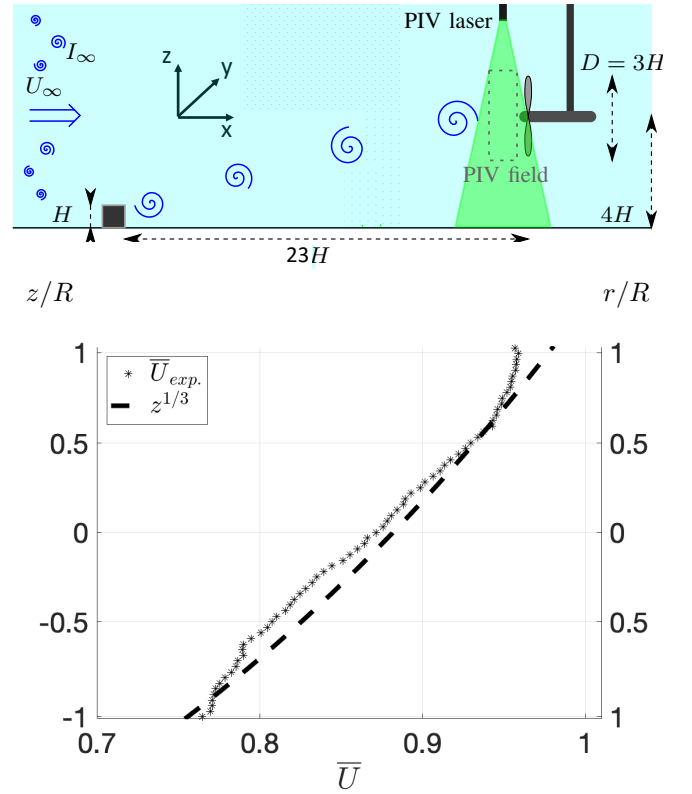


Fig. 7. Top: Illustration in the $y = 0$ symmetrical plane of the experiments. A tidal turbine was located at $x = 23H$ in the wake of the wall-mounted cylinder of height H . $U_\infty = 1$ m/s. The incoming turbulence intensity was $I_\infty = 1.5\%$. Bottom: Mean axial velocity profile at $x = 23H$ without turbine. R , r and z represent the turbine radius, the radial and vertical directions respectively.

in figure 7 (top graph). To mimic the influence of a mean shear that impacts the turbine, a wall-mounted cylinder of dimensions $H \times 6H \times H$ ($H = 0.25$ m) was positioned ahead of the turbine. Particle image velocimetry was performed in front of the rotating turbine to characterize the mean velocity deficit profile in the induction area. The mean axial velocity profile obtained in section $x = 23H$ (the origin is taken at the wall-mounted cylinder, Figure 7 -top graph), without turbine, is plotted in Figure 7 (bottom graph). It satisfies the power law

$$U(z) = U_\infty \left(\frac{z}{D_e} \right)^{1/\alpha} \quad (9)$$

with $\alpha = 3$ and D_e the water depth in the experimental flume tank [3]. Its spatial average over the rotor area is of 0.88 m s^{-1} .

Figure 8 compares the reconstruction as given by (6) with the measured radial component of the velocity field. Overall, the model yields satisfactory results when compared with the experimental database, accurately reproducing the amplitudes, although minor discrepancies are observable at the bottom of the rotor.

C. Discussion

Regardless of whether the incoming flow is uniform or sheared, the modeled and experimental radial velocity components show excellent agreement. The

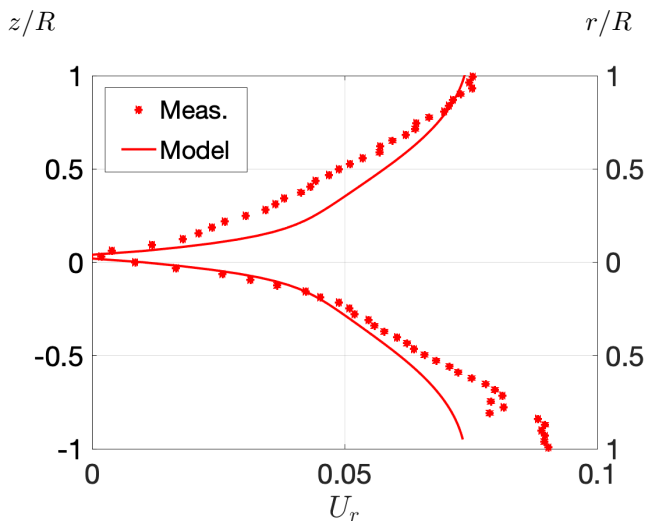


Fig. 8. Mean radial velocity modelling in presence of an incoming shear velocity field. Comparison with experimental data [3]. R , r and z represent the turbine radius, the radial and vertical directions respectively.

modeled radial velocity amplitudes are accurately captured along the diameter of the turbine upstream of the rotating turbine.

Despite some observed differences originating from various sources (including the three-dimensionality of the flow and the limitations of the SSI model near the rotor), one primary distinction arises from the experimental setup. In particular, the boundary conditions at the top and bottom of the water tunnel can significantly impact the flow in front of the rotating turbine. This confined flow likely results in greater tip acceleration than is observed in real-life conditions. Therefore, the specifics of the experimental setup must be considered when comparing modeling predictions with experimental data.

D. 3-D reconstruction

This section illustrates the three-dimensional reconstruction of the radial velocity field. Previously, the axial velocity field (1) was evaluated on a regular Cartesian grid ahead of a rotating turbine for a given thrust coefficient. Equation 6 is then applied to reconstruct the mean radial velocity field in a three-dimensional space. Figure 9 illustrates this reconstruction for three incoming shear flows with a thrust coefficient of $C_t = 0.96$. These radial representations are directly related to the axial representations shown in figure 4.

It is quite interesting to observe that even though the incoming shear velocity profiles are very different, very similar results are obtained. In front of a rotating turbine, the radial velocity does not depend on the incoming velocity shear. This is directly related to the numerical model in which only the axial velocity derivatives are computed. In front of the rotating turbine, the axial flow deceleration remains the same regardless of the velocity amplitude. Consequently, one observes that near the blade's tip, the highest values of the radial velocity are more than 10% of the highest axial velocity values.

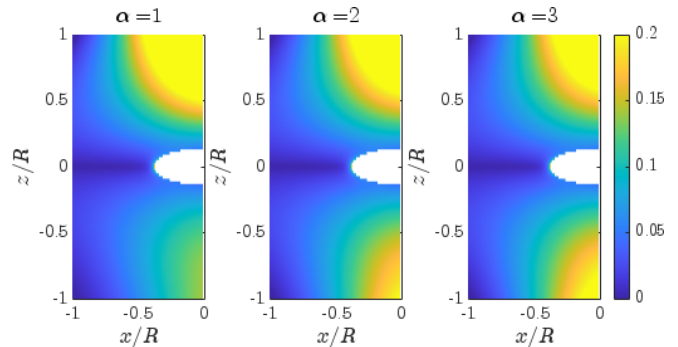


Fig. 9. Two-dimensional representation ($y = 0$ plane) of the mean radial velocity field according to (6). Incoming shear velocity profile $Cz^{1/\alpha}$. $C_t = 0.96$. From left to right: $\alpha = 1$, $\alpha = 2$, and $\alpha = 3$.

Generally, as stated in the introduction part, the contribution of the mean radial velocity is often neglected in several applications. However, such a contribution may help to understand previous observations. For instance, experimental results have clearly demonstrated that wind and tidal turbines in shear flows or inclined angles (such as tilt and yaw) exhibit angular offsets [9], [14]. These offsets are a direct result of pressure differences downstream of the turbine blades, significantly influenced by variations in upstream flow speeds caused by shear and tilt-yaw angles. Corrections for yaw and tilt in BEM theory have been proposed, but adjustments for shear flow, particularly in tidal contexts, remain unclear. The downstream flow of the turbine, which helps us understand the wake produced by the blades, is significantly affected by the conditions of the upstream flow. We expect that our modeling of flow in the induction zone, considering shear flow, will enhance our understanding of the downstream flow from the blades. This improvement will allow us to make future corrections to BEM calculations regarding turbine performance.

IV. CONCLUSION

This paper introduces a novel method for modeling the mean radial velocity component in front of a rotating turbine. Initially, it examines a recent hybrid model designed to reconstruct the three-dimensional mean axial velocity field in front of a rotating tidal turbine under various flow conditions (uniform, shear) and rotational speeds (thrust turbine coefficient). The advantage of present analytical velocity modeling is that it allows a 3D representation of the mean axial velocity field and is able to take into account any vertical shear of the incoming axial velocity field.

Subsequently, using the continuity equation and the axial velocity reconstruction on a three-dimensional meshgrid, the mean radial velocity component is determined. The radial modeling was validated against experimental data under both uniform and shear flow conditions, showing excellent agreement between modeling and experimental results, with minor discrepancies near the blade tips. These differences are likely due to ground effects and the deformable free surface trailing the turbine, which impacts the radial velocity dependence near the blade tips.

The current analytical model does not account for the maximum values observed near the blade tips (90–95% of the chord), where the blade tip vortex is generated. There is a need to enhance the model to address this issue and potentially link these differences to blade geometry or flow environment. Moreover, the axial and radial models have only been validated with experimental data at a constant streamwise position near the hub. New experimental measurements are required to assess the x -dependence in the turbine induction area, which will definitively validate the current models. Similarly, the impact of a wavy environment on alterations in mean axial and radial velocities requires further experimental and analytical investigation.

Improving the model could involve considering the hub's rotational effects. Recent experiments [6] show slight positional shifts in the minimum speed $U_r \sim 0$ around the hub, depending on the thrust coefficients (various Tip Speed Ratios). At rest, $U_r = 0$ is at the hub axis. As the TSR increases, this minimum slightly shifts upward [6]. The interaction between the hub's rotation and the incoming velocity profile likely causes this shift. More detailed radial modeling or new experiments are needed to analyze these complex mechanisms.

To conclude, present analytical axial and radial velocity modelings provide an accurate characterization of the mean velocity deficit and modification in front of a rotating turbine. This modeling allows for a realistic radial distribution of the velocity in the turbine induction area. This would benefit improvement of the numerical modeling of the tidal turbine, similar to the BEM numerical tool, especially in non-uniform inflow conditions [15], [16].

APPENDIX A

THE MODIFIED SELF-SIMILAR INDUCTION MODEL

The initial variant of SSI was introduced and validated through more than 100 Reynolds-averaged Navier-Stokes (RANS) simulations that studied air flow around a porous disk in uniform flow U_{free} [5]. In the turbine induction area, the axial mean velocity $U(r, x)$ is modeled as follows:

$$U(r, x) = U_{\text{free}}(1 + U_{\text{SSI}}(r, x)) \quad (10)$$

where $U_{\text{SSI}}(r, x)$ is the velocity deficit estimated as

$$U_{\text{SSI}}(r, x) = -a_0 \left(1 + \frac{x}{\sqrt{R^2 + x^2}} \right) \text{sech}^{\alpha_1}(\beta\epsilon) \quad (11)$$

with R the rotor radius, a_0 the axial induction factor

$$a_0 = \frac{1}{2} \left(1 - \sqrt{1 - \gamma C_t} \right), \quad (12)$$

and

$$\epsilon = \frac{r}{R\sqrt{\lambda(\eta + x^2/R^2)}}. \quad (13)$$

The constants are set as follows: $\gamma = 1.1$, $\beta = \sqrt{2}$, $\alpha_1 = 8/9$, $\lambda = 0.587$, and $\eta = 1.32$.

To adjust this model to shear inflow conditions, we implemented the following modification:

$$U(r, x, \theta) = U_{\text{free}}(r, x, \theta) + \langle U \rangle U_{\text{SSI}}(r, x) \quad (14)$$

where $\langle U \rangle$ is the spatially averaged velocity over the rotor area, which was also used to compute the thrust coefficient in (12)

$$C_t = \frac{T}{\frac{1}{2}\rho\pi R^2 \langle U \rangle^2}, \quad (15)$$

with ρ , the mass density of the fluid. It should be noted that in Eq. 14, the dependence on the azimuthal coordinate θ arises from the knowledge of U_{free} .

APPENDIX B

THE HUB INDUCTION MODEL

Recently, the effect of nacelle blockage of wind turbines, with particular attention paid to wake flow and loading, has been examined [8]. A simple derivation of the two-dimensional steady velocity field based on the potential velocity ϕ was proposed:

$$U(x, r) = U_{\text{free}} + U_{\text{hub}}(x, r) = U_{\text{free}} + \frac{\partial\phi}{\partial\mu} \frac{\partial\mu}{\partial x} + \frac{\partial\phi}{\partial\xi} \frac{\partial\xi}{\partial x} \quad (16)$$

where (μ, ζ) are semi-elliptic coordinates which are related to the polar coordinates (x, r) as $x = k\mu\xi$ and $r = \sqrt{1 - \mu^2} \sqrt{\xi^2 - 1}$ with $\mu \in [-1, 1]$ and $\xi \in [1, \infty]$, with k the distance from the origin to the foci of the ellipsoid of revolution considered for the modelization of the hub.

APPENDIX C

THE HYBRID INDUCTION MODEL

To assess the mean axial velocity field in front of a rotating tidal turbine, the previously described models have been combined in the following manner:

$$U(x, r, \theta) = U_{\text{free}}(x, r, \theta)(1 + U_{\text{SSI}}(x, r)) + U_{\text{hub}}(x, r). \quad (17)$$

To account for non-homogeneities in the upstream flow such as mean shear, it has been further modified as given in (1). This hybrid induction model has been validated against different incoming shear flow conditions at a fixed streamwise location just in front of a rotating turbine. It has been shown to provide a better description of the mean axial velocity field ahead of a tidal turbine in uniform or sheared inflow conditions [6].

ACKNOWLEDGEMENT

The authors would like to gratefully acknowledge Grégory Germain, Maria Ikhennicheu and Beno t Gaurier (IFREMER, Boulogne-sur-Mer, France) involved in the experimental database previously published ([3], [4], [6], [9]) and used in the present study for comparison and validation of the analytical model.

REFERENCES

- [1] D. Medici, S. Ivanell, J. . Dahlberg, and P.H. Alfredsson, "The upstream flow of a wind turbine: blockage effect", *Wind Energy*, vol. 14, pp. 691–697, 2011.
- [2] M. Bastankhah, and F. Porte-Agel, "Wind tunnel study of the wind turbine interaction with a boundary-layer flow: Upwind region, turbine performance, and wake region," *Phys. Fluids*, vol. 29, no. 065105, 2017.
- [3] Ph. Druault and G. Germain, "Experimental investigation of the upstream turbulent flow modifications in front of a scaled tidal turbine," *Renewable Energy*, vol. 196, pp. 1204–1217, 2022.

- [4] L. Jouenne, Ph. Druault, J.-F. Krawczynski, and G. Germain, "Induction study of a horizontal axis tidal turbine: Analytical models compared with experimental results," *Ocean Eng.*, vol. 268, no. 113458, 2023.
- [5] N. Troldborg and A. Meyer Forsting, "A simple model of the wind turbine induction zone derived from numerical simulations," *Wind Energy*, vol. 20, pp. 2011–2020, 2017.
- [6] Ph. Druault, J.F. Krawczynski, E. Çan and G. Germain "On the necessity of considering the hub when examining the induction of a horizontal axis tidal turbine," *Renewable Energy*, vol. 224, no. 120107, 2024.
- [7] E. Branlard, E. Quon, A. Meyer Forsting, A. Forsting, J. King, and P. Moriarty, "Wind farm blockage effects: comparison of different engineering models," *Journal of Physics: Conference Series*, vol. 1618, no. 6, p. 062036, 2020.
- [8] B. Anderson, E. Branlard, G. Vijayakumar, and N. Johnson, "Investigation of the nacelle blockage effect for a downwind turbine," *J. Phys.: Conf. Ser.*, vol. 1618, no. 062062, 2020.
- [9] B. Gaurier, M. Ikhennicheu, G. Germain, and Ph. Druault, "Experimental study of bathymetry generated turbulence on tidal turbine behaviour," *Renewable Energy*, vol. 156, pp. 1158–1170, 2020.
- [10] M.K. Vinnes, N.A. Worth, A. Segalini, and R. J. Hearst, "The flow in the induction and entrance regions of lab-scale wind farms" *Wind energy*, vol. 26, no 10, pp. 1049-1065.
- [11] D. Medici, S. Ivanell, J.A. Dahlberg, and P.H. Alfredsson, "The upstream flow of a wind turbine: blockage effect" *Wind Energy*, vol. 14, no. 5, pp. 691-697, 2011.
- [12] D. Micallef, G. van Bussel, C. Simao Ferreira and T. Sant, "An investigation of radial velocities for a horizontal axis wind turbine in axial and yawed flows", *Wind Energy* vol. 16, pp. 529-544, 2013.
- [13] H.A. Madsen, C. Bak, M. Dossing, R. Mikkelsen, and S. Oye, "Validation and modification of the blade element momentum theory based on comparisons with actuator disc simulations," *Wind Energy*, vol. 13, no. 4, pp. 373–389, 2010.
- [14] N. Sorensen and J. Johansen . "UpWind: Aerodynamics and aero-elasticity Rotor aerodynamics in atmospheric shear flow", *Proceedings European Wind Energy Conference & Exhibition 2007*.
- [15] H.A. Madsen, V. Riziotis, F. Zahle, M.O.L. Hansen, H. Snel, F. Grasso, T.J. Larsen, E. Politis, and F. Rasmussen, "Blade element momentum modeling of inflow with shear in comparison with advanced model results", *Wind Energy*, vol. 15, no. 1, pp. 63–81, 2012.
- [16] K. Boorsma, J. G. Schepers, G. R. Pirrung, H. A. Madsen, N. N. Sorensen, C. Grinderslev, G. Bangga, M. Imiela, A. Croce and S. Cacciola, "Challenges in Rotor Aerodynamic Modeling for Non-Uniform Inflow Conditions", *J. Phys.: Conf. Ser.* vol. 2767, p. 022006, 2024.